Supporting Information

Ruihao Yuan*[a], Deqing Xue[b], Jinshan Li[a], Dezhen Xue[c], and Turab Lookman[d]

[a] *State Key Laboratory of Solidification Processing, Northwestern Polytechnical Univer- sity, Xi'an 710072, China.*

[b] *School of Materials Science and Engineering, Xi'an University of Technology, Xi'an 710048, China.*

[c] *State Key Laboratory for Mechanical Behavior of Materials, Xi'an Jiaotong University, Xi'an 710049, China.*

[d] *AiMaterials Research, Santa Fe, New Mexico 87501, USA.*

1. All the Features used in the manuscript.

Table S1 All the 18 features used in the manuscript are listed, and the corresponding references for each feature can be found in the supplementary for Ref. 1.

Feature	Description
NCT	the dependence of paraelectric to ferroelectric phase transition temperature on the doping element
NTO	the dependence of tetragonal to orthorhombic phase transition temperature on the doping element
t	tolerance factor calculated by Shannon's ionic radii
tA.B	product of the Shannons's ionic radii of A-site (12-coordination) and B-site (6-coordination) atoms
P	ratio of the polarizability of A-site and B-site elements
p	product of the polarizability of A-site and B-site elements
gr	product of the group of A-site and B-site elements in the element period table
AN	ratio of the atomic number of A-site and B-site atoms in the element period table
EVW	ratio of the equilibrium van der Waals radii of A-site and B-site atoms
evw	product of the equilibrium van der Waals radii of A-site and B-site atoms
AV	ratio of the atomic volume of A-site and B-site atoms
av	product of the atomic volume of A-site and B-site atoms
D	ratio of the ionic displacement of A-site and B-site atoms
ea	product of the ionization energies of A-site and B-site elements
ENP	ratio of the A-site and B-site electronegativity-Pauling scale
enp	product of the A-site and B-site electronegativity-Pauling scale
ENMB	ratio of the A-site and B-site electronegativity-Matyonov Batsanov
enmb	product of the A-site and B-site electronegativity-Matyonov Batsanov

.

We defined the feature for a compound by calculate the ratio/product using elemental features at A-site and B-site, according to equations 1 and 2.

$$ratio = \frac{f_{Ba}X^{Ba}+f_{Ca}X^{Ca}+f_{Sr}X^{Sr}+f_{Cd}X^{Cd}}{f_{Ti}X^{Ti}+f_{Zr}X^{Zr}+f_{Sn}X^{Sn}} \quad (1)$$

$$product = X_A \cdot X_B = (f_{Ba}X^{Ba} + f_{Ca}X^{Ca} + f_{Sr}X^{Sr} + f_{Cd}X^{Cd}) \cdot (f_{Ti}X^{Ti} + f_{Zr}X^{Zr} + f_{Sn}X^{Sn}) \quad (2)$$

Where for example f_{Ba} is the mole fraction for Ba and X^{Ba} represents the value of feature of Ba. The tolerance factor (t) is obtained from equation 3.

$$t = \frac{r_A+r_O}{\sqrt{2}(r_B+r_O)} \quad (3)$$

Where r_A and r_B are the averaged ionic radius of the A-site and the B-site cations, respectively. r_O is the ionic radius of the oxygen anion.

The *NCT* is defined with respect to the change of Curie temperature due to the dopants added to the $BaTiO_3$ matrix. If the doped element decreases the Curie temperature, *NCT* is assigned a value of -1, if the doped element increases the Curie temperature, *NCT* is assigned a value of +1, and if the doped element has no effect on the Curie temperature, *NCT* is assigned a value of 0. For example, the addition of Zr element into the $BaTiO_3$ matrix will decrease the Curie temperature, thus *NCT* of Zr is -1. The *NCT* of a given compound is calculated as the weighted mean using the mole fraction of each element. The definition and calculation for all the 18 features are now described in detail in the supporting information. The definition for *NTO* is similar as *NCT* by considering the influence of dopants on the tetragonal to orthorhombic phase transition temperature.

2. Influence of selected six features on the energy density.

Figures S1(a)-(f) plot the relation between each of the six features and energy density. From the figures we see that there are only very rough correlation between feature and energy density. For example, the value of *NCT* close to -120 gives rise to enhanced energy density, the *av* with a value of ~4100,000 seems beneficial for the energy density. Owing to these poor correlations, the machine learning is in demand

to extract the underlying nonlinear mapping from feature/composition to energy density.

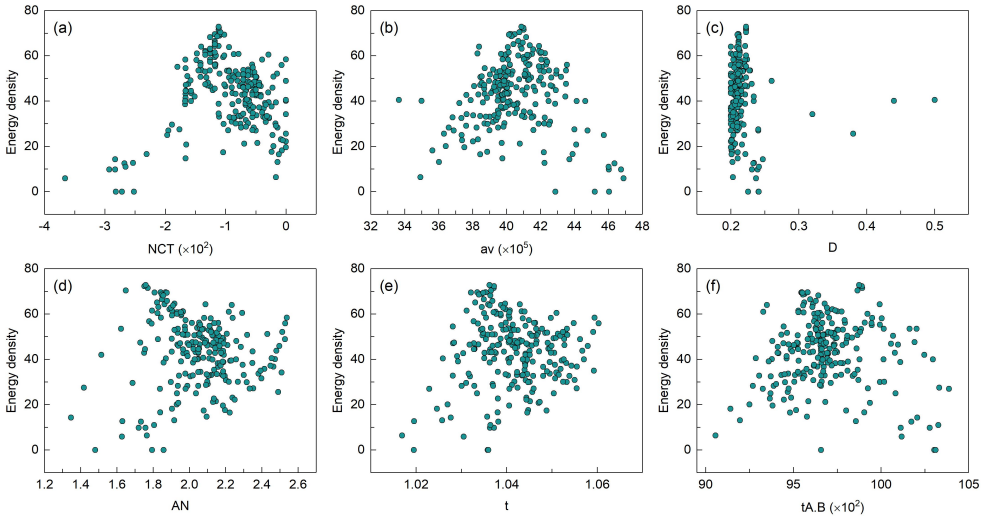

Figure S1 The distribution of energy density as a function of each of the six selected features.

References

1. R. Yuan, Z. Liu, P. V. Balachandran, D. Xue, Y. Zhou, X. Ding, J. Sun, D. Xue and T. Lookman, Adv. Mater., 2018, **30**, 1702884.